



Adsorption kinetics of *diazo-dye* from aqueous solutions by using natural origin low-cost biosorbents

Tuba Sismanoglu, Ayse Z. Aroguz*

Engineering Faculty, Chemistry Department, Istanbul University, Avcilar Campus, Istanbul 24850, Turkey
Tel. +90 212 4737033; email: aroguz@istanbul.edu.tr

Received 7 August 2013; Accepted 16 January 2014

ABSTRACT

In the present study, the adsorption of *diazo-dye* onto natural origin low-cost biosorbents prepared from pyrolyzed petrified sediment (PPS), pyrolyzed sawdust from maple bark and chitin was investigated in aqueous solution. Trypan blue (TrB) was used as *diazo-dye* during the adsorption process. Effects of the operational parameters as contact time and type of adsorbents for the removal of TrB were studied using a batch process. The intraparticle diffusion model, the pseudo-first-order and the pseudo-second-order models were used to examine the kinetic data. Dynamic data of the dye adsorption were also fitted to the intraparticle diffusion model well. The order of the uptaken capacities of dye on these adsorbents was found as chitin > petrified sediment > maple sawdust. Langmuir, Freundlich, Temkin models were employed for fitting the equilibrium adsorption data of TrB. Langmuir and Temkin isotherms were found to represent the data best for the adsorption of TrB onto these adsorbents. The adsorption capacities of the adsorbents PPS, pyrolyzed maple bark sawdust and chitin were obtained to be 345, 72.5, 122 mg g⁻¹ at 298 K, respectively.

Keywords: Adsorption kinetic; Low-cost adsorbent; Petrified sediment; Chitin; Maple bark; *Diazo-dye*

1. Introduction

Many industries as food, textile, plastics, leather, paper, cosmetics widely use dyes to color their products, and they generate huge amount of colored wastewater [1–3]. It is well known that the organic dyestuff is mostly hazardous to human beings and also living organism in aquatic medium. The presence of dyes in the aquatic environment may cause serious pollution problems by reducing light penetration and also prevent from photosynthesis as well as their potential health hazards associated with the carcino-

genic, allergenic, mutagenic and toxic natures. Unlike some of the other pollutants, dyes also cause esthetic pollution and eutrophication [2,3]. The literature reports indicate numerous techniques for the removal of dye pollutants from wastewater [4–6]. Some of these methods are biological treatment, coagulation, filtration, microfiltration, oxidation, sedimentation, flotation, adsorption, ion exchange, reverse osmosis and electrolysis [6–9]. Among these techniques, adsorption is the most effective method for removing dyestuff pollutants from wastewater [6–10]. Ali et al. [4] reported that the cost of water treatment of these technologies (except adsorption) ranged from 10 to 450 US\$/m³ of treated water. Depending on the ease

*Corresponding author.

of operation and the selection of low-cost adsorbents, adsorption is considered as the best wastewater treatment technique. Because of its microporous structure, high adsorption capacity and extraordinary surface area activated carbon is commonly used for the removal of dyes and pigments from wastewater [10]. But it is expensive and it has regeneration problems. Therefore, many researchers continue their work to find out low cost and easily obtainable materials for adsorption process. A large number of natural materials such as, peanut hull [2], natural sediments [3,11], bentonite [12], moss peat [13], wheat bran [14], seashell [15], rice husk [16], wood and wood sawdust [17,18], tree bark [19,20] and chitin [21–24] were studied as the effective adsorbents. Among these materials, considerable attention has recently been paid to the adsorption of dyes from aqueous solutions using the bark sawdust produced from different sources. These materials are produced in large quantities as byproducts which causes disposal problems in the furniture industry. It is known from the literature that a huge amount of maple wood sawdust is also produced in the wood industries [17–19,25]. Maple wood sawdust was found highly effective adsorbent for the adsorption of copper (II) ions from aqueous solutions [25].

Chandrasekaran and Shin suggested a new method for the color removal process for azo dyes as trypan blue (TrB) in the industrial wastewater using aminopropyl-functionalized magnesium phyllosilicate [26]. TrB is mainly used in paper industry, and it is considered as chemical carcinogens. Therefore, before discharge into the receiving medium, TrB requires to be removed from the wastewater.

In this work, the pyrolyzed petrified sediment (PPS), the pyrolyzed maple bark (PMB) and chitin were used as the adsorbents and their adsorption feasibilities in the batch system were studied for TrB as *diazo-dye*. The experimental data were modeled using Langmuir, Freundlich and Temkin isotherms. The kinetic data obtained from the batch adsorption process were analyzed using the pseudo-first-order kinetic, second-order kinetic and intraparticle diffusion models for the adsorption of TrB.

2. Materials and methods

2.1. Materials

TrB was purchased from Sigma–Aldrich Company and used as received. It was chosen as a model dye in this study because it is a blue vital dye having fine color properties to selectively color dead tissues or cells blue. One of the major applications of TrB is to

dye and print leather and cotton. It is known as diamine blue that contains two azochromophores. TrB is harmful by inhalation and ingestion, and it is cancer suspect agent if it is absorbed through the skin. The maximum absorbance value of TrB was measured at the wavelength of 595 nm. The chemical structure of TrB ($C_{34}H_{24}N_6Na_4O_{14}S_4$) is shown in Fig. 1(a) [27]. The other chemicals used in this work as NaOH, HCl were from Merck and used without further purification.

2.2. Preparation of adsorbents

Petrified sediment was collected from Cape Cod, USA. Maple bark was also obtained from Amherst, USA. Both of them were washed and dried 110°C for 2 h. Before being used as adsorbents, they were separately pyrolyzed in a ceramic boat placed in a stainless steel tubular reactor with 220 mm length and 75 mm internal diameter. The pyrolyzation temperature was 900°C, and pyrolyzation time was 1 h. The heating rate was kept of 15°C min⁻¹. The temperature was adjusted by using a Ni–Cr–Ni thermocouple. After being pyrolyzed, the samples were allowed to cool down to room temperature, under a N₂-flow. The samples were then washed with hot distilled water and dried at 110°C until becoming constant in weight. The pyrolyzed materials were ground and sieved through a 200-mesh screen. The specific surface areas of the PPS and the PMB were measured using BET technique (Branauer–Emmett–Teller nitrogen adsorption) with Micrometrics' FlowSorb II-2300 and found 28.1 and 12.4 m² g⁻¹, respectively. The pyrolyzed adsorbents were stored in a desiccator for further experimentation. Chitin [poly(N-acetyl-1,4-β-D-glucopyranosamine)] ($C_8H_{13}NO_5$)_n used in this study having the molecular weight M_r 400,000 was supplied from Fluka. The molecular structure of chitin is seen in Fig. 1(b).

2.3. Batch adsorption experiments

Batch adsorption experiments were carried out in 25 cm³ glass flasks containing 0.1 g of natural adsorbents and 10 cm³ of TrB with the concentration of 1 g dm⁻³. Fresh solutions were used for each experiment. Our preliminary results indicated that the maximum uptaken of TrB took place at pH 7.5. Therefore, pH of the working solutions was adjusted to 7.5 by either 0.1 N NaOH or 0.1 N HCl solutions. All the adsorption experiments were conducted in the temperature controlled water bath. During the adsorption process, the samples were taken at the pre-determined time intervals and separated the adsorbents from the

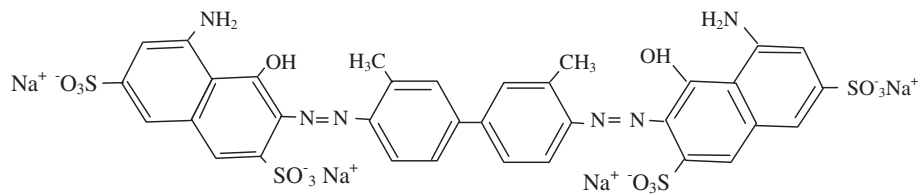


Fig. 1(a). The chemical structure of TrB.

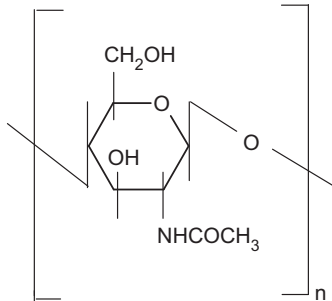


Fig. 1(b). The molecular structure of chitin.

solution by centrifugation at 3,000 rpm at 20 min. Change of the concentration of TrB in the resultant solution was subsequently determined by CHEBIOS optimum-one UV–visible spectrophotometer with 1.0 cm path-length cell at 595 nm wavelength. The difference between the concentrations of TrB in the aqueous solutions before and after adsorption gives the adsorbed amount of TrB on the adsorbents. Each experiment was duplicated under identical conditions, and a negative control (without adsorbent) was simultaneously carried out to ensure that the sorption was caused by the adsorbents and not by the container. The uptake percent of TrB by the adsorbents was estimated by using the following expressions,

$$\% \text{ Uptake} = (C_0 - C) \times \frac{100}{C_0} \quad (1)$$

where C_0 (mgL^{-1}) is the initial concentration of TrB and C represents C_t and C_e which are the concentration of TrB (mg L^{-1}) in the solution at time t and at equilibrium, respectively. The mass of TrB adsorbed per unit mass of the adsorbents (q) at any time ($C = C_t$) and at equilibrium ($C = C_e$) was calculated from Eq. (2).

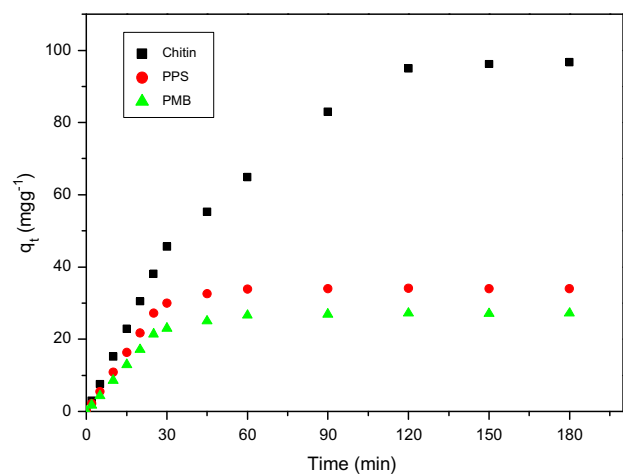
$$q = (C_0 - C) \frac{V}{W} \quad (2)$$

q is the adsorbed amount of TrB in the solid phase at equilibrium ($q = q_e$) and time t (min) ($q = q_t$), respectively. V indicates the volume of dye solution in L and W is the weight (g) of the adsorbent.

3. Results and discussion

3.1. Effect of contact time on adsorption behavior

The removal of TrB by the adsorbents as a function of contact time is shown in Fig. 2. According to this figure, two stages of adsorption were observed for all the adsorbents. Effect of the contact time on the adsorption capacity (q_t) was observed a number of quick increases during the first 5–30 min which showed the rapid adsorption and slow adsorption followed by the gradual increase during the adsorption process. The slow adsorption stage was obtained during 30–60 min for the adsorbents PPS and PMB and 30–120 min for the chitin. The adsorbed amount of TrB on these three adsorbents rose with increasing time and reached the plateau value at about 60 min for PPS and PMB. The equilibrium of adsorption was established in two hours for the adsorption of TrB on chitin. The uptake percent of TrB by PPS and PBM was

Fig. 2. Dynamics of TrB uptake by chitin, PPS and PMB at 25 ± 1 °C, pH 7.5.

34 and 27%, respectively. The adsorption of TrB on chitin was also found 96%.

3.2. Kinetic modeling

Kinetic study of the adsorption of TrB from aqueous solution onto the adsorbents was carried out by the well-known Lagergren's pseudo-first-order, pseudo-second-order and intraparticle models.

3.2.1. Pseudo-first-order model

Pseudo-first-order rate expression is given as [28]:

$$\frac{dq_t}{dt} = k_1(q_e - q_t) \quad (3)$$

Integrating of Eq. (3). for the boundary conditions at $t = 0, q_t = 0$ and $t = t, q_t = q_t$ gives the following equation.

$$\ln(q_e - q_t) = \ln q_e - k_1 t \quad (4)$$

where k_1 is the pseudo-first-order rate constant of the adsorption (min^{-1}). Pseudo-first-order kinetic for the TrB on the adsorbents PPS, PMB and chitin plotted at 25°C is given in Fig. 3. From this figure, Lagergren's first-order rate constant (k_1) and adsorption capacity (q_e) were calculated from the slope and the intercept of the plot, respectively. Table 1 shows these values with the corresponding correlation coefficients. The results reveal that the correlation coefficients, R^2 , have high values 0.97, 0.96 and 1 for the adsorbents of PPS, PMB and chitin, respectively. The high values of the correlation coefficients of the first-order kinetics model indicate the applicability of this kinetic equation on the adsorption process of TrB by the adsorbents used in this work. The calculated q_e values for all adsorbents are much closer to the experimental q_e in the case of pseudo-first-order kinetic model. These results verify the adequacy of the pseudo-first-order model.

3.2.2. Pseudo-second-order model

The pseudo-second-order kinetic model is analyzed by Ho and McKay based on the adsorption capacity and is expressed as follows [29]:

$$\frac{t}{q_t} = \frac{1}{h} + \frac{t}{q_e} \quad (5)$$

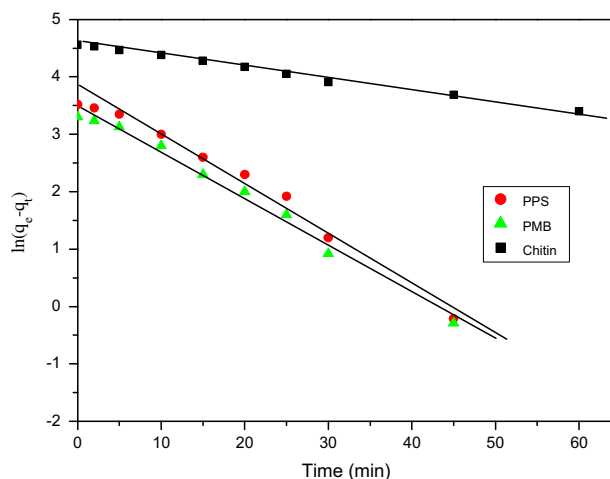


Fig. 3. Pseudo-first-order model for the adsorption of TrB by chitin, PPS and PMB at $25 \pm 1^\circ\text{C}$.

$$h = k_2 q_e^2 \quad (6)$$

where h ($\text{mg g}^{-1} \text{min}^{-1}$) is the initial adsorption rate, k_2 ($\text{g mg}^{-1} \text{min}^{-1}$) is the equilibrium rate constant of pseudo-second-order adsorption and q_e (mg g^{-1}) is the equilibrium adsorption capacity. The values of k_2 and q_e can be determined experimentally from the slope and intercept of the plot of t/q_t vs. t , respectively. The results are given in Fig. 4 and in Table 1. The correlation coefficients, R^2 , are found low values for the adsorbents PPS, PMB and chitin. The experimental values of $q_{e,\text{exp}}$ do not comply with the calculated values $q_{e,\text{cal}}$ for the second-order kinetic model. This result shows that the second-order kinetic model does not fit well with the whole range of contact time. As seen in Table 1, the correlation coefficients of pseudo-first-order kinetic are much higher than in the case of pseudo-second-order kinetic model.

3.2.3. Intraparticle diffusion model and adsorption mechanism

When the adsorption process occurs in the porous of adsorbents and the internal resistance to diffusive transport process is much higher than the external resistance, this kind of adsorption process is called intraparticle diffusion. Intraparticle diffusion process is often considered as the rate-limiting step in many adsorption processes, and through the intraparticle diffusion, the adsorbate is most probably transported from the bulk of the solution into the adsorbent phase. The intraparticle diffusion model is proposed by

Table 1
Kinetic parameters for the removal of TrB by PPS, PMB and chitin at 298 K

Adsorbents	$q_{e,exp}$ (mg g^{-1})	Pseudo-first order			Pseudo-second order		Intraparticle				
		k_1 (min^{-1})	$q_{e,calc}$ (mg g^{-1})	R^2	k_2 ($\text{g mg}^{-1} \text{min}^{-1}$)	$q_{e,calc}$ (mg g^{-1})	R^2 ($\text{g mg}^{-1} \text{min}^{-1/2}$)	$k_{i,1}$ ($\text{g mg}^{-1} \text{min}^{-1/2}$)	R^2 ($\text{g mg}^{-1} \text{min}^{-1/2}$)	$k_{i,2}$ ($\text{g mg}^{-1} \text{min}^{-1/2}$)	R^2
PPS	34.2	8.60×10^{-2}	42.1	0.96	2.53×10^{-4}	71.9	0.82	2.30	0.92	6.95	0.98
PMB	27.2	8.10×10^{-2}	31.2	0.97	3.19×10^{-4}	56.8	0.82	5.54	0.98	6.95	0.99
Chitin	95.3	1.97×10^{-2}	95.5	1.00	1.62×10^{-4}	108.7	0.8	10.5	0.97	1.71	1.00

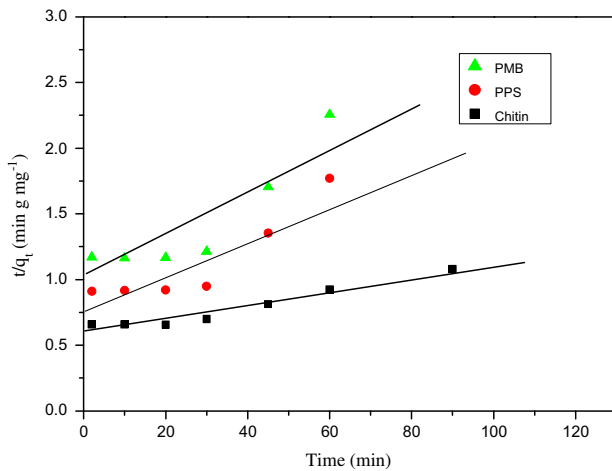


Fig. 4. Pseudo-second-order model for the adsorption of TrB by chitin, PPS and PMB at 25 ± 1 °C.

Weber and Morris to analyze the mechanism of the adsorption. This model is expressed as follows [30]:

$$q_t = k_i t^{1/2} + C \quad (7)$$

where k_i is the intraparticle diffusion rate constant ($\text{mg g}^{-1} \text{min}^{-1/2}$). C (mg g^{-1}) gives an idea about the boundary layer thickness. According to Eq. (7), the straight line of the plot of q_t vs. $t^{1/2}$ shows that the adsorption follows the intraparticle diffusion process. The slope of the straight line and the intercept give the values k_i and C , respectively. Here, when the values of C equal to zero, then the plot passes through the origin. The intraparticle diffusion is the sole rate-limiting step. The linear plot represents that intraparticle diffusion plays a significant role in the removal of TrB. As seen from Fig. 5, the plots cannot pass through the origin. Therefore, it is not the sole rate-controlling step, although intraparticle diffusion is involved in the adsorption system. Two linear portions can be observed from the graph in Fig. 5. The

first line indicates boundary layer effect, and the following line shows intraparticle or pore diffusion. These two lines demonstrate that the adsorption process proceeds by surface sorption and then the intraparticle diffusion. The rate constants of intraparticle diffusion, $k_{i,1}$ and $k_{i,2}$, are obtained from the slope of the first and second linear portion of the plot. The calculated intraparticle diffusion coefficients $k_{i,1}$ and $k_{i,2}$ values are shown in Table 1. This data show that the adsorption mechanism of TrB on these adsorbents also follows the intraparticle diffusion model.

The mechanism for the removal of TrB may be assumed to involve the following four steps. In the first step, dye migrates from bulk solution to the surface of the adsorbent. In the second step, dye diffuses to the surface of the adsorbent. The adsorption of dye at an active site on the surface of the adsorbents was observed at the third step. At the last step, intraparticle diffusion of dye into the interior pores of the adsorbent particles was seen. The results of the intraparticle diffusion model confirm that the adsorption of the TrB on the adsorbents was a

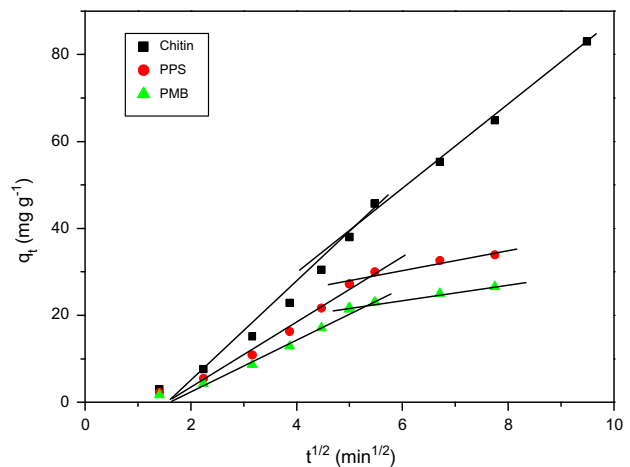


Fig. 5. Intraparticle diffusion kinetics of TrB onto chitin, PPS and PMB at 25 ± 1 °C.

multi-step process which involves adsorption on the external surface then diffusion into the interior of the pores.

3.3. Adsorption isotherms

The adsorption of TrB onto the adsorbents chitin, PPS and PMB was studied with the commonly used models, Langmuir, Freundlich and Temkin isotherms.

3.3.1. The Freundlich isotherm

The adsorption data of TrB were also analyzed by using the Freundlich isotherm model. This model was used for the heterogeneous systems and represented as [31]:

$$q_e = K_F C_e^{\frac{1}{n}} \tag{8}$$

where K_F and n are Freundlich constants related to adsorption capacity and adsorption intensity, respectively. The linear form of Freundlich isotherm is expressed by the following equation,

$$\log q_e = \log K_F + \frac{1}{n} \log C_e \tag{9}$$

where C_e is the equilibrium concentration in the solution (mg dm^{-3}). As seen from Fig. 6(a), the

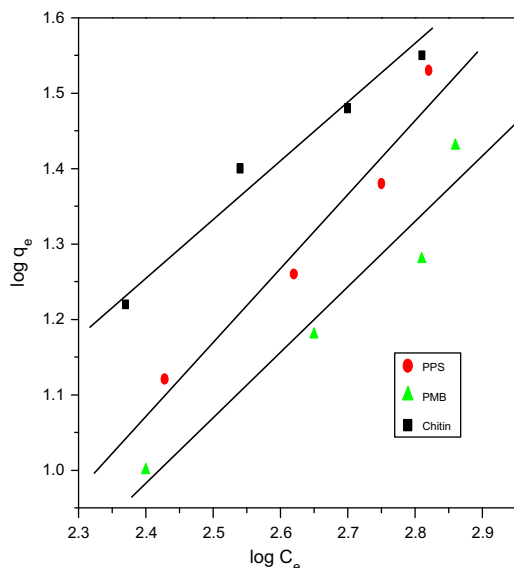


Fig. 6(a). The Freundlich isotherm model for the adsorption of TrB on PPS, PMB and chitin at 25 ± 1 °C.

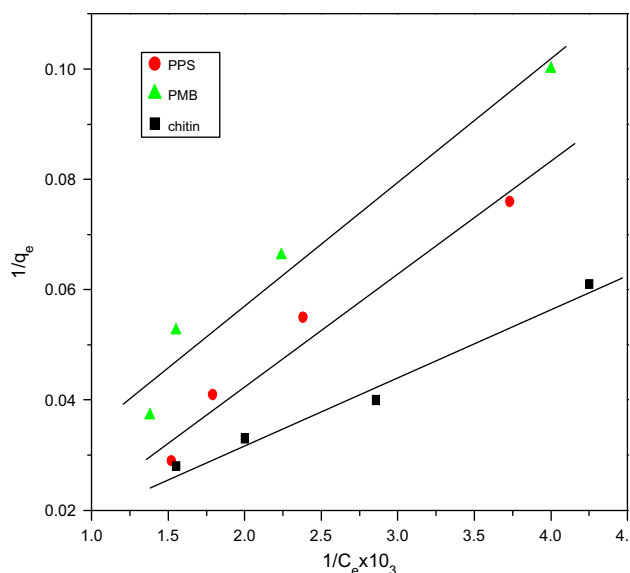


Fig. 6(b). The Langmuir isotherm model for the adsorption of TrB on PPS, PMB and chitin at 25 ± 1 °C.

Freundlich isotherm constants of K_F and n for each adsorbent are determined from the intercept and the slope of the linear plot of $\log C_e$ vs. $\log q_e$, respectively. These constants are experimental constants (in Table 2), and they are determinative of the extent of the adsorption and the degree of nonlinearity between solution concentration and the adsorption, respectively.

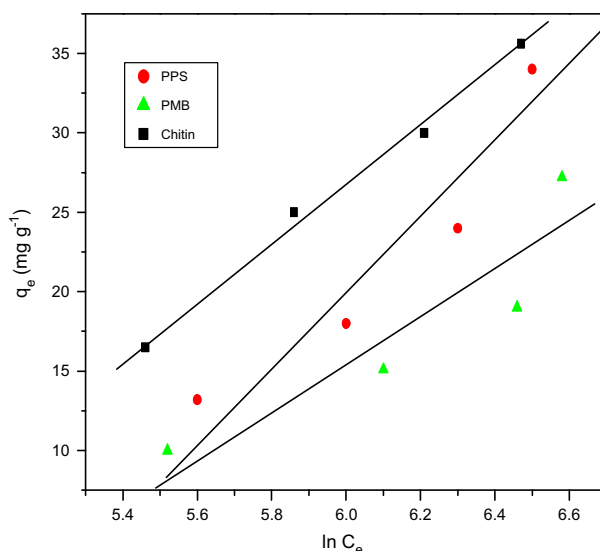


Fig. 6(c). The Temkin isotherm model for the adsorption of TrB on PPS, PMB and chitin at 25 ± 1 °C.

Table 2

Freundlich, Langmuir and Temkin isotherm constants for adsorption of TrB on PPS, PMB and chitin

Adsorbents	Langmuir			Freundlich			Temkin		
	q_m (mg g^{-1})	K_L ($\text{dm}^3 \text{g}^{-1}$)	R^2	K_F ($\text{dm}^3 \text{g}^{-1}$)	n	R^2 ($\text{dm}^3 \text{g}^{-1}$)	A ($\text{g mg}^{-1} \text{min}^{-1/2}$)	B	R^2
PPS	345	0.144	0.96	3.64	1.02	0.95	1.22	110	0.90
PMB	72.5	0.63	0.96	2.82	1.19	0.94	1.23	68	0.84
Chitin	122	0.68	0.98	1.66	1.37	0.97	1.25	84	0.99

3.3.2. The Langmuir isotherm

The linear form of the Langmuir equation is expressed as [32]:

$$\frac{1}{q_e} = \frac{1}{q_m} + \frac{1}{(q_m K_L)} C_e \quad (10)$$

where C_e (mg L^{-1}) is the equilibrium concentration of TrB in solution, q_e (mg g^{-1}), the amount of TrB adsorbed per gram of the adsorbents, K_L (L mg^{-1}) is the Langmuir constant related to the energy of adsorption. q_m is the maximum adsorption capacity with complete monolayer coverage on the adsorbent surface (mg g^{-1}). The values listed in Table 2 are determined from the slopes and intercept of the linear plot of $1/C_e$ vs. $1/q_e$, respectively, as seen in Fig. 6(b). In this model, it is assumed that the adsorption occurs at a specific homogeneous surface of the adsorbent. In order to predict the adsorption efficiency of the process, the dimensionless constant is determined by using the following equation:

$$r = \frac{1}{(1 + K_L C_0)} \quad (11)$$

where C_0 is the initial concentration (mg dm^{-3}) and K_L is the Langmuir constant. The values of r between 0.0 and 1.0 represent the favorable adsorption of the adsorbate. Values of $r > 1$ represent unfavorable adsorption. The values of dimensionless parameter, r , for the adsorption of TrB on PPS, PMB and chitin are found to be 0.87, 0.61 and 0.60, respectively. These values obtained between 0.0 and 1.0 indicate that the adsorption of TrB on the adsorbents used in this work is highly favorable. By comparing the results of correlation coefficient in Table 2, it can be seen that Langmuir model yields better fit than Freundlich model. The results of Langmuir isotherm reveal that TrB adsorption follows monolayer adsorption.

3.3.3. Temkin isotherm

The linearized form of Temkin isotherm is given as follows;

$$q_e = B \ln K_T + B \ln C_e \quad (12)$$

where B and K_T (L g^{-1}) are Temkin constants. Temkin isotherm shows a strong affinity for the adsorption capacity of TrB on the adsorbents. Temkin isotherm is based on two assumptions [33]. The first assumption is related to the heat of adsorption of the molecules in the layer which decreases linearly with the coverage due to the interactions between adsorbate and adsorbent. The second assumption shows the uniform distribution of the binding energies.

A plot of C_e vs. q_e gives the isotherm constants B and K_T from the slope and intercept, respectively. K_T is the equilibrium binding constant corresponding to the maximum binding energy and B related to the heat of adsorption. Based on the correlation coefficients (R^2) (Table 2), the results showed that good applicability was also obtained by Temkin isotherm as seen in Fig. 6(c).

4. Conclusions

The adsorption of *diazo-dye*, TrB on PPS, PMB and chitin has been investigated in batch model. The adsorption equilibrium time was found 60 min for PPS and PMB and 2 h for chitin. The adsorption of TrB was best described by pseudo-first-order kinetic model. The adsorption of TrB on these adsorbents complied with the intraparticle diffusion kinetic model. Batch model adsorption studies followed both Langmuir and Temkin adsorption isotherms. Chitin was found very effective adsorbent with the maximum uptake percentage of 96% for TrB. The uptaken percent of TrB by PPS and PBM was obtained 34% and 27%, respectively. The use of PPS, PMB can also be alternative for the high cost adsorbents due to its low cost and quite good efficiency for TrB.

References

- [1] A. Mittal, D. Kaur, J. Mittal, Batch and bulk removal of a triarylmethane dye, Fast Green FCF, from wastewater by adsorption over waste materials, *J. Hazard. Mater.* 163(2–3) (2009) 568–577.
- [2] R. Gong, M. Li, C. Yang, Y. Sun, J. Chen, Removal of cationic dyes from aqueous solution by adsorption on peanut hull, *J. Hazard. Mater.* 121(1–3) (2005) 247–250.
- [3] A.Z. Aroguz, J. Gulen, R.H. Evers, Adsorption of methylene blue from aqueous solution on pyrolyzed petrified sediment, *Bioresour. Technol.* 99(6) (2008) 1503–1508.
- [4] I. Ali, M. Asim, T.A. Khan, Low cost adsorbents for the removal of organic pollutants from wastewater, *J. Environ. Manage.* 113 (2012) 170–183.
- [5] I. Ali, V.K. Gupta, Advances in water treatment by adsorption technology, *Nature* 1 (2006) 2661–2667.
- [6] I. Ali, Water treatment by adsorption columns: Evaluation at ground level, *Sep. Purif. Rev.* 43 (2014) 175–205.
- [7] I. Ali, New generation adsorbents for water treatment, *Chem Rev.* 112 (2013) 5073–5091.
- [8] Y. Çöpür, A. Tozluoglu, M. Özkan, Evaluating pretreatment techniques for converting hazelnut husks to bioethanol, *Bioresour. Technol.* 129 (2013) 182–190.
- [9] A. Bennani, B. Karim, M. Mounir, M. Hachkar, M. Bakasse, A. Yaacoubi, Removal of basic red 46 dye from aqueous solution by adsorption onto moroccan clay, *J. Hazard. Mater.* 168(1) (2009) 304–309.
- [10] S. Karaca, A. Gürses, M. Açıkyıldız, M. Ejder (Korucu), Adsorption of cationic dye from aqueous solutions by activated carbon, *Micropor. Mesopor. Mat.* 115(3) (2008) 376–382.
- [11] Q.H. Tao, H.X. Tang, Effect of dye compounds on the adsorption of atrazine by natural sediment, *Chemosphere* 56 (2004) 31–38.
- [12] G. Bereket, A.Z. Aroguz, M.Z. Özel, Removal of Pb (II), Cd(II), Cu(II), and Zn(II) from aqueous solutions by adsorption on bentonite, *J. Colloid Interface Sci.* 187(2) (1997) 338–343.
- [13] Y.S. Ho, G. McKay, The kinetics of sorption of divalent metal ions onto sphagnum moss peat, *Water Resour.* 34(3) (2000) 735–742.
- [14] M.T. Sulaka, C.H. Yatmaz, Removal of textile dyes from aqueous solutions with eco-friendly biosorbent, *Desalin. Water Treat.* 37 (2012) 169–177.
- [15] J. Gulen, A.Z. Aroguz, D. Dalgın, Adsorption kinetics of azinphosmethyl from aqueous solution onto pyrolyzed horseshoe sea crab shell from the Atlantic Ocean, *Bioresour. Technol.* 96(10) (2005) 1169–1174.
- [16] M.C. Shih, Kinetics of the batch adsorption of methylene blue from aqueous solutions onto rice rusk: Effect of acid-modified process and dye concentration, *Desalin. Water Treat.* 154(1–3) (2012) 337–346.
- [17] Y.S. Ho, G. McKay, Kinetic models for the sorption of dye from aqueous solution by wood, *Institute of Chemical Engineers, Trans. I Chem. E.* 76 (1998) 183–193.
- [18] F.K. Bangash, S. Alam, Adsorption of acid blue 1 on activated carbon produced from the wood of *Ailanthus altissima*, *Braz. J. Chem. Eng.* 26(2) (2009) 275–285.
- [19] L.C. Morais, E.P. Gonçalves, L.T. Vasconcelos, C.G.G. González Beça, Reactive dyes removal from wastewaters by adsorption on eucalyptus bark—Adsorption equilibria, *Environ. Technol.* 21(5) (2000) 577–583.
- [20] R. Saliba, H. Gauthier, R. Gauthier, M. Petit-Ramel, The use of eucalyptus barks for the adsorption of heavy metal ions and dyes, *Adsorpt. Sci. Technol.* 20 (2) (2002) 119–129.
- [21] T. Şişmanoğlu, Removal of some fungicides from aqueous solution by the biopolymer chitin, *Colloid Surface A* 297(1–3) (2007) 38–45.
- [22] G. Annadurai, L.Y. Ling, J.F. Lee, Adsorption of reactive dye from an aqueous solution by chitosan: Isotherm, kinetic and thermodynamic analysis, *J. Hazard. Mater.* 152(1) (2008) 337–346.
- [23] Z. Bekçi, C. Özveri, Y. Seki, K. Yurdakoç, Sorption of malachite green on Chitosan bead, *J. Hazard. Mater.* 154(1–3) (2008) 254–261.
- [24] H. Karaer, I. Uzun, Adsorption of basic dyestuffs from aqueous solution by modified chitosan, *Desalin. Water Treat.* 51 (2013) 2294–2305.
- [25] M.S. Rahman, M.R. Islam, Effects of pH on isotherms modeling for Cu(II) ions adsorption using maple wood sawdust, *Chem. Eng. J.* 149(1–3) (2009) 273–280.
- [26] G. Chandrasekaran, H.J. Shin, Monitoring color removal of trypan blue by AMP clay, *J. Biosci. Bioeng.* 108 (2009) S75–S95.
- [27] S. Shrestha, Y.S. Shim, K.C. Kim, K.H. Lee, H. Cho, Evans blue and other dyes as protein tyrosine phosphatase inhibitors, *Bioorg. Med. Chem. Lett.* 14(8) (2004) 1923–1926.
- [28] S. Lagergren, Zur theorie der sogenannten adsorption gelöster stoffe [About the theory of so-called adsorption of soluble substances], *Kungliga Svenska Vetenskapsakademiens Handlingar*, Band 24(4) (1898) 1–39.
- [29] Y.S. Ho, G. McKay, Pseudo-second order model for sorption processes, *Process Biochem.* 34(5) (1999) 451–465.
- [30] W.J. Weber, J.C. Morris, Kinetics of adsorption on carbon from solution, *J. Sanit. Eng. Div. Am. Soc. Civil Eng.* 89 (1963) 31–60.
- [31] H.M.F. Freundlich, Über die adsorption in lösungen, *Z. Phys. Chem.* 57A (1906) 385–470.
- [32] I. Langmuir, The adsorption of gases on plane surfaces of glass, mica and platinum, *J. Am. Chem. Soc.* 40(9) (1918) 1361–1403.
- [33] M.I. Temkin, V. Pyzhev, Kinetics of ammonia synthesis on promoted iron catalysts, *Acta Physicochim URS* 12 (1940) 327–356.